J Wood Sci (2014) 60:105–110
DOI 10.1007/s10086-013-1381-z

ORIGINAL ARTICLE

Density calculation of wood by portable X-ray tube with consideration of penetrating depth

Chul-Ki Kim · Jung-Kwon Oh · Jung-Pyo Hong · Jun-Jae Lee

Received: 3 September 2013 / Accepted: 6 November 2013 / Published online: 20 December 2013

Abstract A portable X-ray apparatus generates soft X-rays which have a continuous wavelength (wide range). When using continuous wavelength X-rays, the mass attenuation coefficient of the soft X-rays is changed as the penetrating depth in wood increases, unlike monochromatic X-rays which are usually used for medical purposes. In safety inspections of historic buildings, penetrating depth varies in an X-ray radiograph. Computerized tomography (CT) is a powerful tool that helps determine the density information of the inner sections of buildings. Because only portable X-rays can be used in historic buildings and the penetrating depth can vary, the mass attenuation coefficient of wood according to penetrating depth needs to be investigated. Therefore, in this study, we developed a statistical method which takes into account the influence of the penetrating depth on a density calculation made by a portable X-ray apparatus. X-ray tests were conducted on wood specimens of various depths. From the results, a statically determined mass attenuation coefficient (SMAC) ($\mu = -0.214\ln(t) + 0.7251$), which is the equation of mass attenuation coefficient according to the penetrating depth in wood, was derived to convert radiographs to density radiographs. All projections were converted into density profiles using two methods, average mass attenuation coefficient and SMAC. Based on the density profile for each projection, a density distribution of a cross-section was reconstructed by filtered back projection. Compared with the cases using a consistent mass attenuation coefficient, SMAC provided much higher precision in density prediction than the average mass attenuation coefficient.

Keywords Mass attenuation coefficient · Soft X-ray · Continuous wavelength X-ray · Density CT image · Portable X-ray apparatus

C.-K. Kim
Department of Forest Sciences, Seoul National University, 6218 200 Bldg., 1 Gwanak-ro, Gwanak-gu, Seoul, Korea

J.-K. Oh
Department of Forest Sciences, Research Institute for Agriculture and Life Sciences, Seoul National University, 6218 200 Bldg., 1 Gwanak-ro, Gwanak-gu, Seoul, Korea

J.-P. Hong
Wood Engineering Team, SK Forest co. Ltd., 4F Baeksang Bldg., 197-28 Gwanhun-dong, Jongno-gu, Seoul, Korea

J.-J. Lee (✉)
Department of Forest Sciences, Research Institute for Agriculture and Life Sciences, Seoul National University, 6221 200 Bldg., 1 Gwanak-ro, Gwanak-gu, Seoul, Korea
e-mail: junjae@snu.ac.kr

Introduction

Northeast Asia including Korea, Japan and China has a number of wooden structures which have survived over many generations. These cultural properties can be damaged by living organisms (wood-rotting fungi, termites) or environmental factors (ultraviolet rays, moisture) [1]. Schmidt [2] also reported that heartwood can be damaged by fungi which can considerably affect the strength and volume reduction of the tree xylem. Detecting the biodeteriorations caused by a living organism is especially difficult because they usually begin at the inner part of the wood. Moreover, the biodeteriorations can affect physical properties or quality of wood by reducing wood density, which is one of the most important properties of wood.

In order to detect the internal state of wood, non-destructive testing (NDT) has been developed. Divos and

Divos [3] showed that the resolution of acoustic tomography using stress waves was influenced by the wavelength of the stress waves and the number of sensors. Nicolotti et al. [4] reported that ultrasonic tomography with a frequency of 54 kHz was a very effective tool for the detection of internal decay when compared to electric or georadar tomography. They successfully detected internal decay using acoustic techniques, although the techniques could not provide the inner density distribution.

Compared with these acoustic techniques, X-rays have higher resolution when used to evaluate the inner state of wood. Moreover, X-rays can provide density information. To verify wood density, research on X-ray attenuation in wood has been conducted for several decades. Olson et al. [5] calculated the change of mass attenuation coefficient according to tube voltage for conifer wood. The ideal X-ray energy between 5.13 and 5.69 keV for 1 mm thick wood samples provided the maximum attenuation difference between earlywood and latewood. Nakada et al. [6, 7] used soft X-ray imaging to study the MC distribution in clear Japanese cedars according to direction. In addition to density distribution, X-rays can provide the size/location of a defect when computed tomography (CT) is used in conjunction. The X-ray CT image can be reconstructed using numerous radiographs obtained with a rotating X-ray apparatus. Macedo et al. [8] reported that CT image quantification in terms of dry bulk density could be obtained for three different X- and gamma-ray energies (28.3, 59.5 and 662.0 keV). Lindgren et al. [9] reconstructed a density CT image of clear wood to determine the physical properties in three directions (radial, tangential and longitudinal direction). Moberg [10] and Oja and Temnerud [11] analyzed CT images to locate internal knots and resin pockets, which can be used to increase the production yield of lumber.

Despite the advantages of X-ray techniques, X-ray and CT techniques are difficult to use in the field where structures or trees are located. The equipment is more suitable for laboratory tests, and radiation shields have been installed to prevent inspectors from hazardous radiation. However, installation of the radiation shield in the test field is difficult. Additionally, the level of radiation intensity is too dangerous to use without a radiation shield. Thus, the first step in solving the field applicability problem was using soft X-rays from a portable X-ray apparatus. Positioning oneself a sufficient distance from the X-ray source could reduce the risk of radiation exposure when not using a radiation shield if low-energy intensity X-rays (soft X-rays) were used. Moreover, low-energy intensity X-rays can be generated by a portable X-ray tube which is commercially produced for NDT or security inspections.

The attenuation behavior of soft X-rays is different from that of the hard X-rays used in previous studies. Attenuation of soft X-rays is governed by the penetrating depth of the object as well as its density, because soft X-rays from a portable apparatus have a continuous wavelength. Longer wavelengths tend to be attenuated by scattering rather than absorption, and in a thicker object, attenuation is more likely to be affected by scattering [12]. The effect of penetrating depth on density prediction for soft X-rays was investigated in this study, and the result of density CT images was presented using the attenuation behavior of soft X-rays.

Materials and methods

Materials

Two sets of specimens were prepared in this study; the first set was prepared for determination of mass attenuation coefficient, and the second set for the validation of CT reconstruction, which uses a different mass attenuation coefficient according to penetrating depth.

For determination of mass attenuation coefficient according to penetrating depth, small specimens of four different wood species were prepared: cedar (*Cryptomeria japonica*), larch (*Larix leptolepis*), pitch pine (*Pinus rigida*), and Korean pine (*Pinus koraiensis*). Table 1 shows the size, density and moisture contents of approximately ten specimens for each species.

For the second test setup, a round wood with an artificial hole was prepared to confirm the accuracy of the CT image. The species of round wood was pitch pine, and its air-dried density and moisture content were 430 kg/m^3 and 12 %, respectively. Figure 1a, b shows schematic drawings of the round wood.

Methods

X-ray apparatus

The X-ray tube K-4 (Softex, Japan) with a maximum tube voltage and current of 60 kV and 5 mA, respectively, was used in this study.

Table 1 Details of specimens for four wood species

Species	Size (mm)[a]			Density (kg/m^3)[b]		MC (%)
	Width	Height	Length	Ave	SD	
Cedar	31.51	33.37	80.00	328.07	40.66	12
Larch	32.87	38.58		460.93	74.70	
Pitch pine	31.50	33.58		505.11	26.63	
Red pine	32.90	39.95		410.11	37.13	

Width, height and length was radial, tangential and longitudinal direction, respectively

[a] Average dimension for ten specimens for each species

[b] Air-dry density at MC 12 %

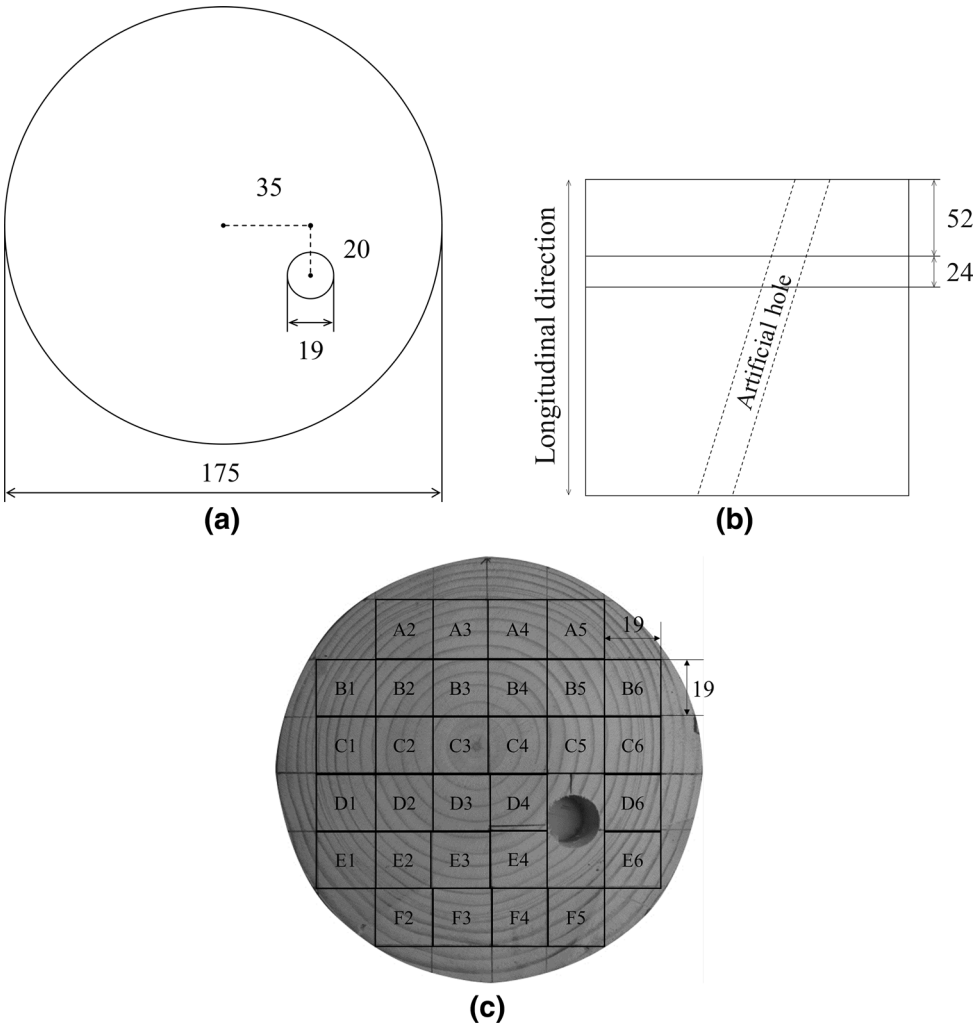

Fig. 1 Round wood with an artificial hole for CT image reconstruction (unit mm). **a** Diameter and location of the artificial hole in the top of the round wood, **b** location of disk 24 mm in height to verify the accuracy of the CT image in the side view of the round wood, **c** location of small specimens to measure air-dry density in the top of the disk using the dimension method

The digital detector NX 06 (RF System, Japan), composed of scintillators and 12 charge-coupled devices (CCDs) combined into one unit, was used to obtain radiographs. The maximum resolution of the digital detector was approximately 319 pixels/mm^2. The portable X-ray apparatus was installed at the CT location designed for laboratory-scale tests.

Based on the experience of previous on similar size of objects inspections, an X-ray intensity of 37 kV and 2 mA was chosen. The specific wood area was irradiated for 5 s, the digital detector compiled the exposure data, and digitalized JPG files were automatically saved in a laptop computer.

Derivation of mass attenuation coefficient according to penetrating depth of soft X-rays in wood

As Fig. 2 shows, the penetrating depth was changed by changing the number of wood blocks of which information was in Table 1. The intensity of transmitted X-rays reportedly decreases exponentially if the beam is a collimated monochromatic beam [13] (Eq. 1), and Eqs. 2 and 3 can be derived from Eq. 1 as follows:

$$I = I_0 e^{-\mu\rho t} \quad (1)$$

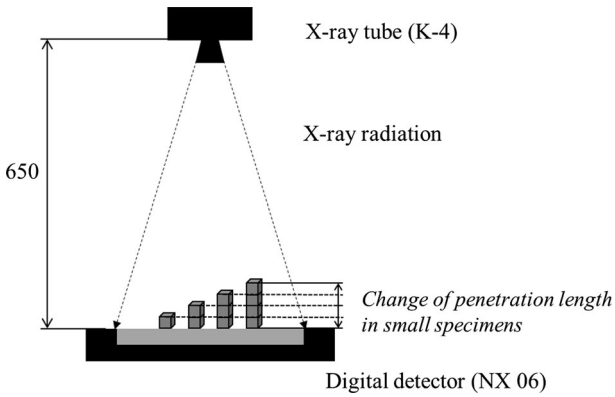

Fig. 2 Schematic diagram of the test for the mass attenuation coefficient using four species of wood (unit mm)

$$\ln(I) = -\mu\rho t + \ln(I_0) \quad (2)$$

$$\rho = \frac{\ln(I_0/I)}{\mu t} \quad (3)$$

where I is the intensity of the transmitted soft X-ray (mSv), I_0 is the intensity of the initial soft X-ray (mSv), ln is the natural log, μ is the mass attenuation coefficient (cm^2/g), ρ is the air-dry density (g/cm^3), and t is the soft X-ray penetrating depth in the wood (cm).

Linear regression was used to predict the mass attenuation coefficient from Eq. 2. A residual was defined as the difference between the actual value of the dependent variable and the value predicted by the linear model,

$$r_i = y_i - f(x_i) \quad (4)$$

where r_i is a residual, y_i is a dependent value ($\ln(I)$), $f(x_i) = \beta_1 x_i + \beta_2$ is the linear regression model, β_1 and β_2 are coefficients of regression, and x_i is wood mass per unit area of the ith specimen (g/cm^2) and represents the product of density and thickness (ρt).

Two types of mass attenuation coefficients were derived, a constant mass attenuation coefficient (μ) and a mass attenuation coefficient according to penetrating depth ($\mu(t)$).

The constant mass attenuation coefficient was determined as β_1 as the minimum sum of squared residuals for all pieces of clear wood block.

To determine mass attenuation coefficients according to penetrating depth ($\mu(t)$), 88 values were divided into nine groups according to the penetrating depth, which was the sum of wood block thickness penetrated by the X-rays. For each group, a mass attenuation coefficient was determined in the same manner as the constant mass attenuation coefficient. This procedure was repeated for each group. Finally, nine mass attenuation coefficients were determined according to the penetrating depth. Using regression analysis, the nine coefficients were expressed as Eq. 5 below:

$$\mu = -a \log(t) + b \quad (5)$$

where a and b are coefficients of the regression equation.

This equation and the constant mass attenuation coefficients were used to convert radiographs into density profiles.

Reconstruction of density CT images and accuracy verification

To reconstruct the density CT image, 180 radiographs were taken as the round wood was rotated 2° at a time during the CT scanning. Using the constant mass attenuation coefficient and the logarithmic regression equation for mass attenuation, the 180 radiographs were converted into two sets of 180 density profiles. Subsequently, the CT images were reconstructed by a filtered back projection (FBP) algorithm program and Matlab R2007 (Mathworks Inc., Natick, MA, USA).

To verify the accuracy of the two density CT images, the round wood was cut into a disk 24 mm in height, and the disk was cut into 30 small specimens, as shown in Fig. 1c. The air-dry density of the 30 small specimens was evaluated using the dimension method. Then, the evaluated air-dry density was compared with the estimated density value in the two density CT images to verify the accuracy.

Results and discussion

Mass attenuation coefficient according to penetrating depth in clear wood

As shown in Fig. 3, the mass attenuation coefficient for the four species of wood was 0.1844 for the entire wood block. However, the mass attenuation coefficient decreased as the soft X-rays penetrating depth in wood increased. This result indicated that the quantity of transmitted soft X-rays

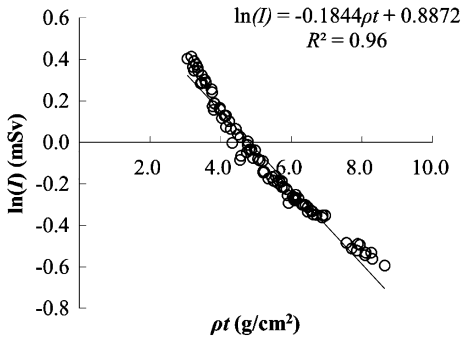

Fig. 3 Mass attenuation coefficients for all pieces of the wood block (ρt is wood mass per unit area, I is the intensity of the transmitted soft X-ray)

Table 2 Mass attenuation coefficient (MAC) according to penetrating depth in wood

Penetrating depth (cm)				MAC (cm^2/g)	R^{2b}
Ave	Max	Min	CV[a]		
6.50	6.29	6.58	0.020	0.3218	0.97
6.72	6.71	6.73	0.001	0.3045	0.99
7.78	7.69	7.98	0.008	0.3018	0.99
9.45	9.44	9.47	0.001	0.2515	0.99
9.87	9.85	9.98	0.003	0.2332	0.99
12.60	12.59	12.62	0.001	0.1854	0.98
13.15	13.14	13.17	0.001	0.1572	0.98
15.72	15.36	15.99	0.015	0.1386	0.99
16.44	16.42	16.46	0.001	0.1241	0.99

[a] Coefficient of variation = standard deviation/ave

[b] Coefficient of determination for mass attenuation coefficient

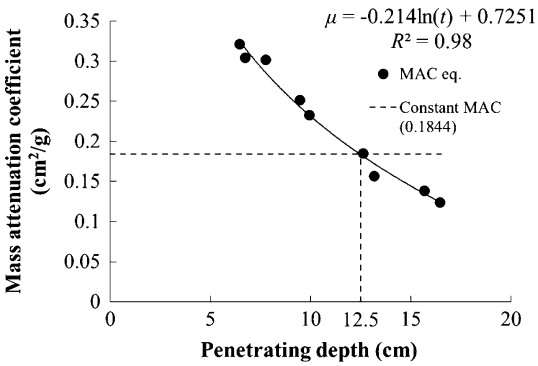

Fig. 4 Mass attenuation coefficient (MAC) according to soft X-ray penetrating depth in wood

increased as the penetrating depth increased because the intensity of X-rays was attenuated by scattering as well as absorption when the penetrating depth was large [12]. Therefore, the soft X-ray intensity of scattering as well as transmitting was considered by using each penetrating depth to derive the mass attenuation coefficient. Table 2 and Fig. 4 show the mass attenuation coefficient of the soft X-rays according to the penetrating depth in wood.

As a result, a logarithmic regression equation of the mass attenuation coefficient according to penetrating depth in wood was determined as Eq. 6 below:

$$\mu = -0.214\ln(t) + 0.7251 \quad (6)$$

The coefficient of determination (R^2) of the regression was 0.98. The equation was used to convert radiographs into density profiles because, if the constant mass attenuation coefficient did not reflect the soft X-ray intensity including scattering and absorption, the accuracy of estimating the density would be too high. The equation was also applicable at 12 % MC because this technique was carried out for historic wooden properties which will be kept near an air-dry MC.

Verification of density CT image accuracy

A set of 180 density radiographs was taken while rotating the round wood 2° at a time during CT scanning. Density profiles were constructed with two different mass attenuation coefficients; the first coefficient was a constant mass attenuation coefficient (0.1844 cm^2/g) derived without consideration of penetrating depth, and the other was the function regarding penetrating depth (Eq. 6), derived as 3.1.

Based on the two sets of 180 density profiles, two individual density CT images which clearly showed the location of pith, annual ring and artificial hole were reconstructed as shown in Fig. 5. The density CT images were compared with the air-dry density, as shown in Fig. 1c. The constant mass attenuation coefficient (Fig. 5a)

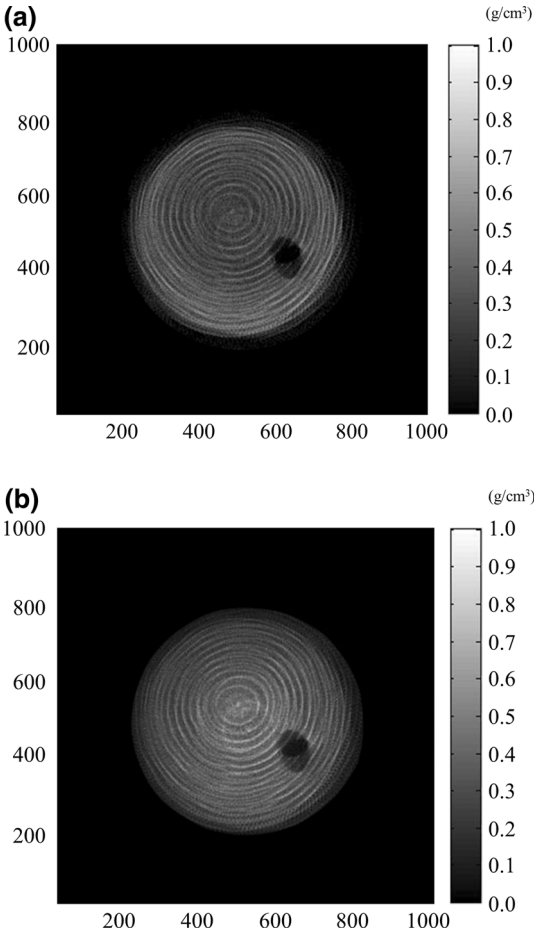

Fig. 5 Density CT image using the mass attenuation coefficient. **a** Reconstructed CT image using a constant mass attenuation coefficient, 0.1844, **b** reconstructed CT image using the equation of mass attenuation, $\mu = -0.214\ln(t) + 0.7251$

underestimated the air-dry density in the specimen's midsection; however, the density of the exterior sections was overestimated, which apparently was caused by the effect of the penetrating depth on the mass attenuation coefficient. The value of the constant mass attenuation coefficient, 0.1844 cm^2/g, was similar to the wood at a depth of 125 mm as shown Fig. 4. Because the penetrating depth through the sections was shorter, as shown Fig. 6, the density of the exterior sections of specimens was overestimated when the constant mass attenuation coefficient (0.1844 cm^2/g) was used, as it was smaller than the actual value. The root mean square error (RMSE) of all the small specimens was 165 kg/m^3, and the RMSE of the midsection was smaller than that of the exterior sections (RMSE, midsection 82 kg/m^3, exterior sections 209 kg/m^3).

When using the equation of mass attenuation coefficient in the density CT image (Fig. 5b), RMSE for all the small specimens was 41 kg/m^3, and RMSEs for the midsection and exterior sections were 12 and 54 kg/m^3, respectively. The prediction accuracy of round wood density was

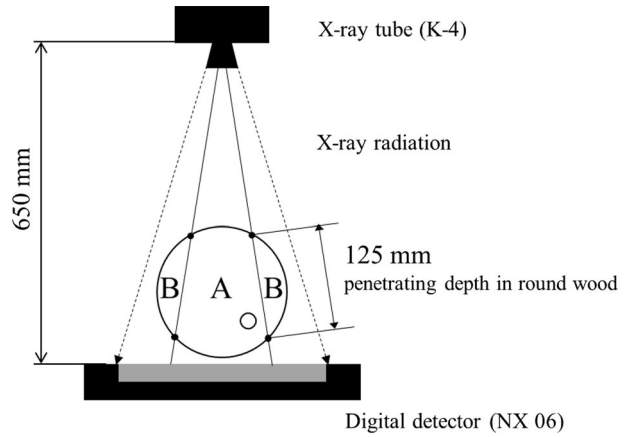

Fig. 6 The estimated parts according to penetrating depth, using constant mass attenuation coefficient (*A* underestimated midsection, *B* overestimated exterior part)

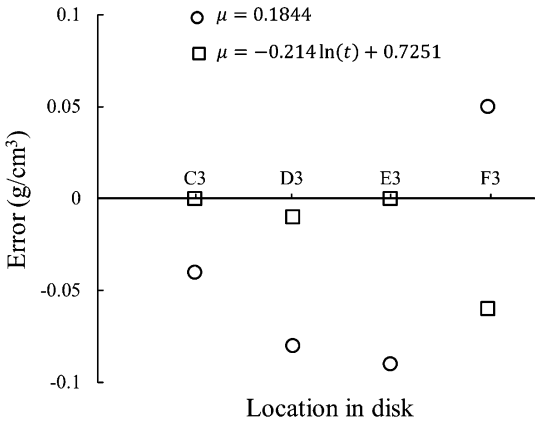

Fig. 7 Comparison between air-dry density using the dimension method and the estimated density using CT images (*C3–F3* refer to Fig. 1c). Error = estimated density using CT images−air-dry density measured by dimension method

improved, as shown in Fig. 7. However, the exterior sections of the round wood were underestimated because the digital detector could not measure the X-ray attenuation passing through the short penetrating depth with high precision. Thus, the exterior sections of specimen were underestimated.

Although the estimation accuracy for the exterior section of the specimens was not particularly good, the overall estimated density distribution was properly evaluated using the portable X-ray equipment with X-rays of low intensity and continuous wavelength, demonstrating its usefulness in the on-site detection of deterioration such as heart rot or termite damage.

Conclusion

In this study, we investigated the effects of penetrating depth on attenuation of soft X-rays to reconstruct density CT images and application of the X-ray CT technique in the field. The results showed the mass attenuation coefficient of the soft X-rays decreased as the penetrating depth increased, and the mass attenuation coefficient was presented as a function of penetrating depth, $\mu = -0.214\ln(t) + 0.7251$ at 12 % MC.

Using this equation, a set of 180 radiographs was converted into density profiles, and a CT image was reconstructed. When density in the CT images was compared with air-dry density measured by the dimension method, the RMSE of prediction was 41 kg/m^3, showing a much lower RMSE of prediction than when not considering the influence of penetrating depth on attenuation.

From this study, the CT technique using soft X-rays was improved sufficiently for use in inspecting wood or standing trees, which can be damaged by various factors such as heart rot and termites.

Acknowledgments This study was supported by the Bio-industry Technology Development Program (project No. 111054-3), Ministry of Agriculture, Food and Rural Affairs.

References

1. National research institute of cultural heritage (2012) Conservation of wooden objects. Pointtech, Daejeon, p 8
2. Schmidt O (2010) Wood and fungi. Springer, Heidelberg, pp 53–54
3. Divos F, Divos P (2005) Resolution of stress wave based acoustic tomography. In: 14th international symposium on nondestructive testing of wood, Shaker, Germany, pp 307–314
4. Nicolotti G, Socco LV, Martinis R, Godio A, Sambuelli L (2003) Application and comparison of three tomographic techniques for detection of decay in tree. J Arboric 29(2):66–78
5. Olson JR, Liu CJ, Tian Y, Shen Q (1988) Theoretical wood densitometry: II. Optimal X-ray energy for wood density measurement. Wood Fiber Sci 20(1):187–196
6. Nakada R, Fujisawa Y, Hirakawa Y (1999) Soft X-ray observation of water distribution in the stem of *Cryptomeria japonica* D. Don I: general description of water distribution. J Wood Sci 45(3):188–193
7. Nakada R, Fujisawa Y, Hirakawa Y (1999) Soft X-ray observation of water distribution in the stem of *Cryptomeria japonica* D. Don II: types found in wet-area distribution patterns in transverse sections of the stem. J Wood Sci 45(3):194–199
8. Macedo A, Vaz CMP, Pereira JCD, Naime JM, Cruvinel PE, Crestana S (2002) Wood density determination by X- and gamma-ray tomography. Holzforschung 56(5):535–540
9. Lindgren O, Davis J, Wells P, Shadbolt P (1992) Non-destructive wood density distribution measurements using computed tomography. Holzforschung 50(7):295–299
10. Moberg L (2000) Models of internal knot diameter for *Pinus sylvestris*. Scand J For Res 15(2):177–187
11. Oja J, Temnerud E (1999) The appearance of resin pockets in CT-images of Norway spruce (*Picea abies* (L.) Karst.). Holzforschung 57(5):400–406
12. Korean society of physics for radiosurgery (2005) Radiation physics (in Korean). Komoonsa, Seoul, pp 209–211
13. Kaelbel EF (1967) Handbook of X-rays. McGraw-Hill, New York, pp 41(3)–41(24)